Electronic Supplementary Information

Theoretical and Experimental Insights into the Effects of Halogen Composition on the Thermal-Decomposition Details, as well as the Fire-Suppressing Mechanism and Performance of $CF_3CX{=}CH_2$ (*X* = F, Cl, Br)

Suting Zhou, Qi Yang, Haijun Zhang,* Xiaomeng Zhou*

Center for Aircraft Fire and Emergency, Department of Safety Engineering, Civil Aviation University of China, Tianjin 300300, P. R. China.

To whom correspondence should be addressed. Email: hjzhang_ahu@163.com (HZ) zhouxm@nankai.edu.cn (XZ)

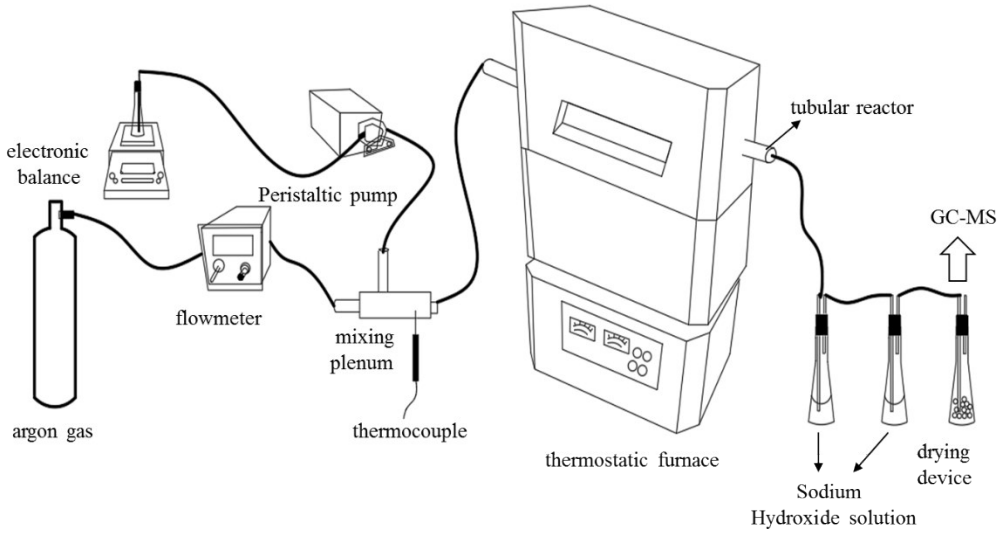

Figure S1. The diagram of experimental equipment for thermal decomposition.

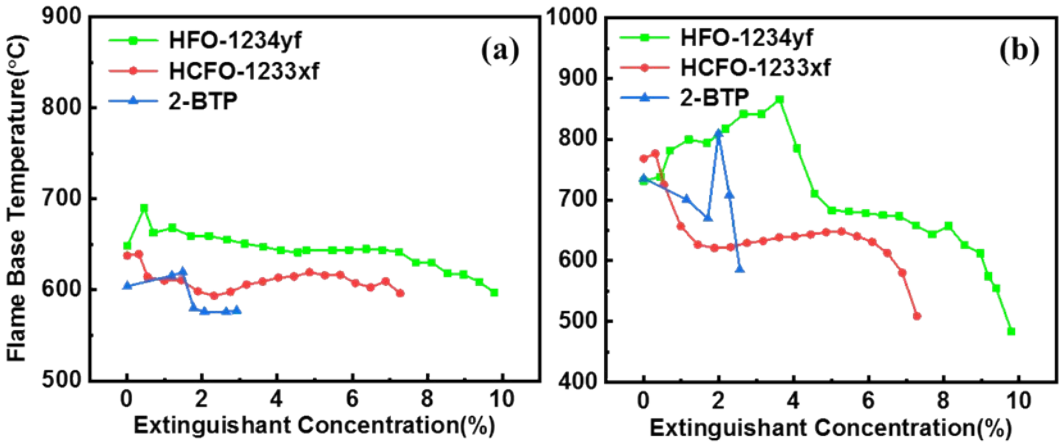

Figure S2. The temperature of flame root for (a) propane and (b) methane flame at different concentration of extinguishant.

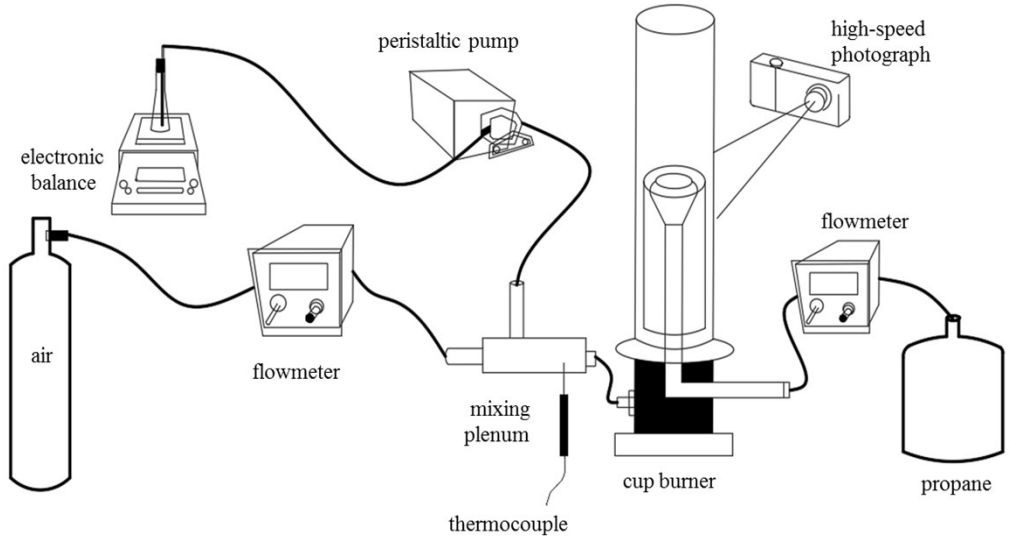

Figure S3. The diagram of experimental device for cup-burner measurement.

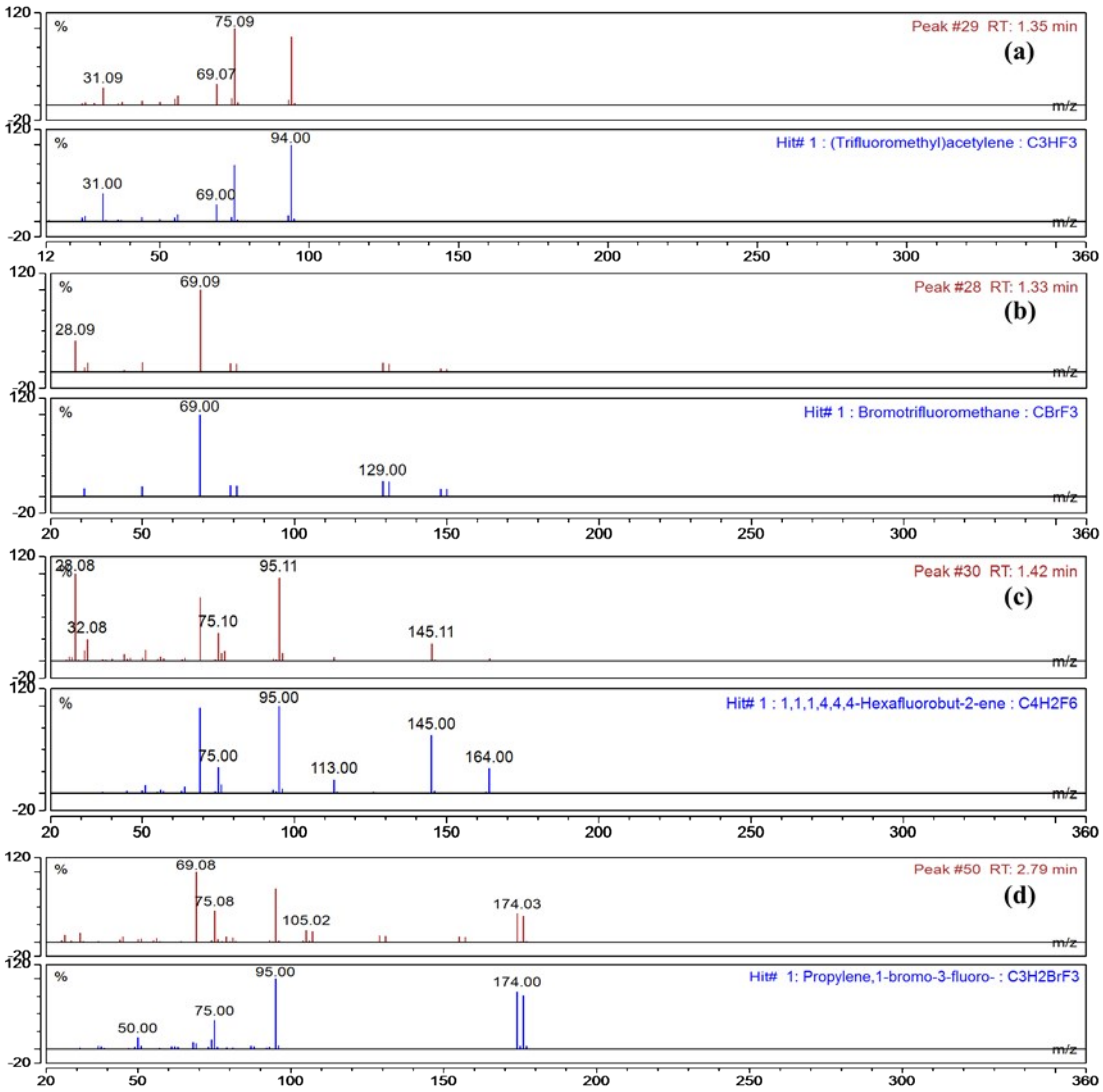

Figure S4. The mass spectra of (a) $CF_3C{\equiv}CH$, (b) CF_3Br, (c)$C_4H_2F_6$ and (d) $C_3H_2F_3Br$.

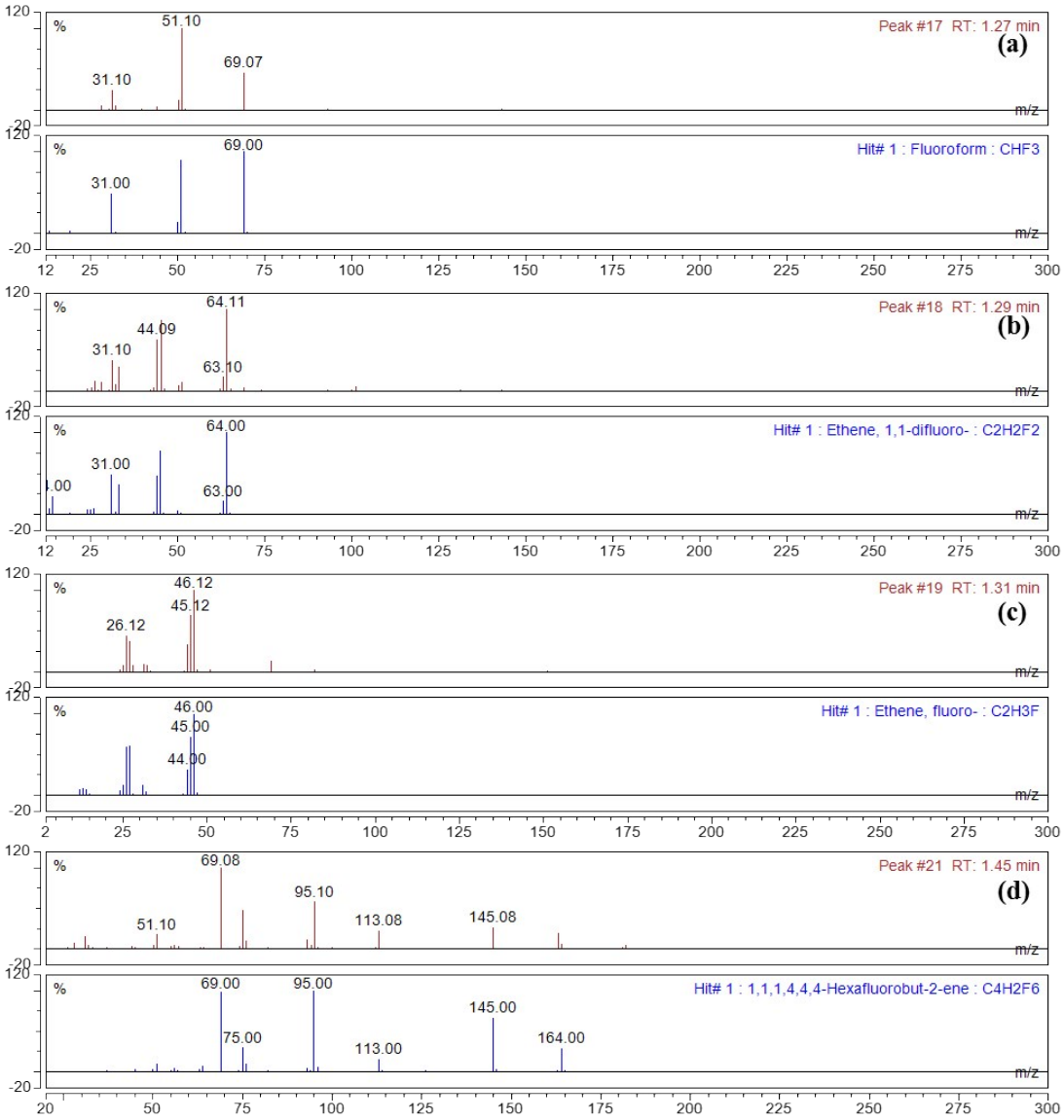

Figure S5. The mass spectra of (a) CF_3H, (b) $C_2H_2F_2$, (c) C_2H_3F and (d) $C_4H_2F_6$.

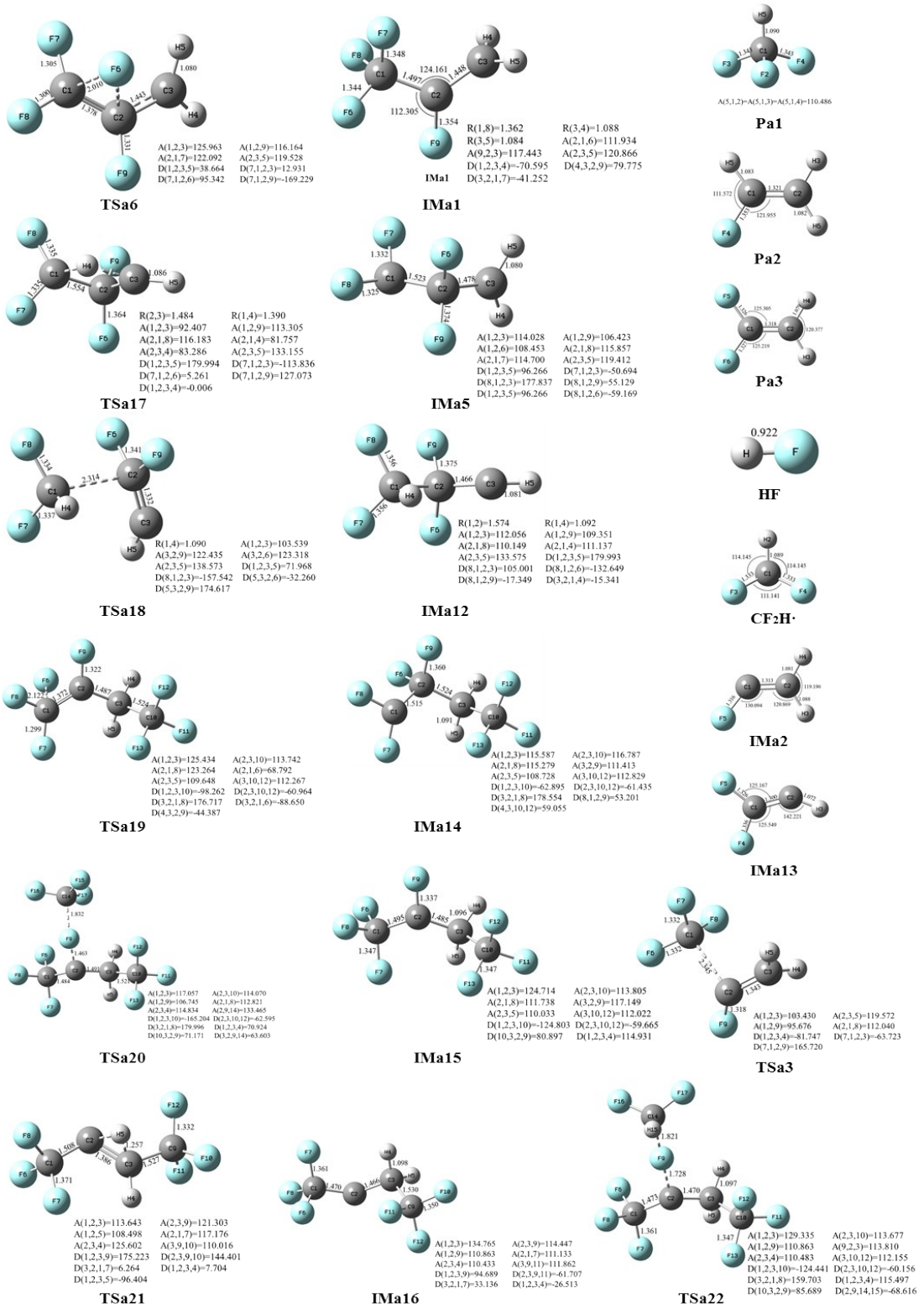

Figure S6. Geometric structures of main products, transition states and intermediate products in the optimal decomposition path of HFO-1234yf.

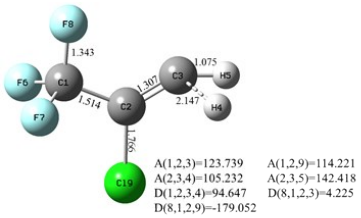

TSb3

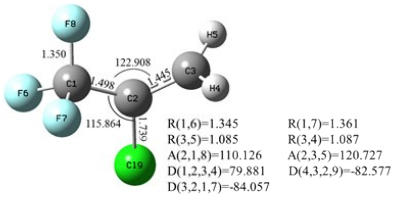

IMb1

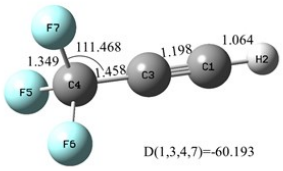

Pb1/Pc1

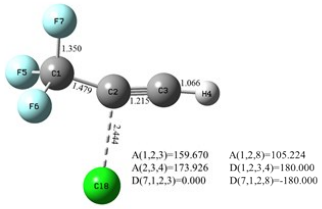

TSb7

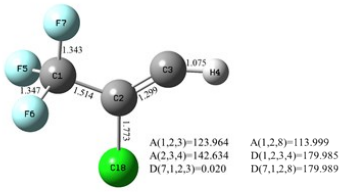

IMb3

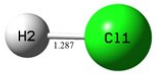

HCl

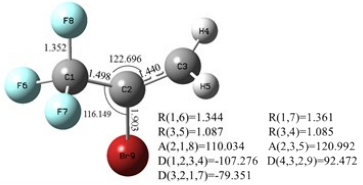

IMc1

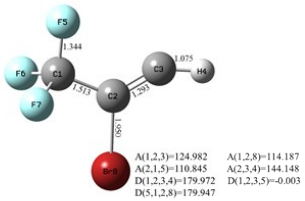

IMc2

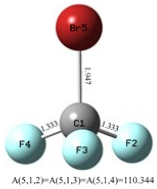

Pc2

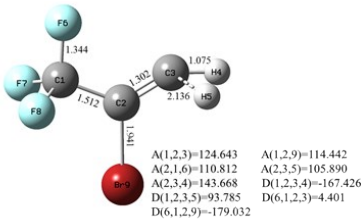

TSc3

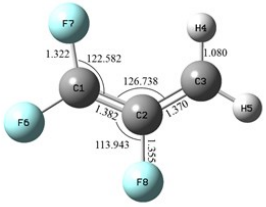

IMc3

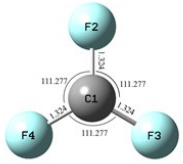

CF3·

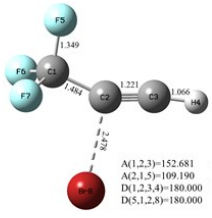

TSc8

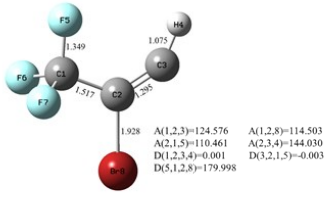

IMc5

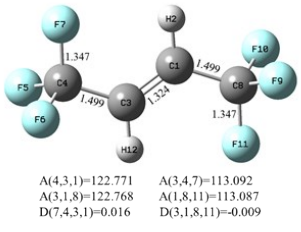

Pc3-1

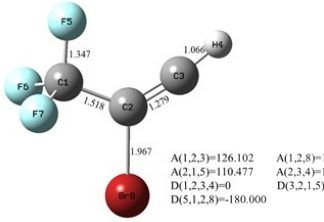

TSc9

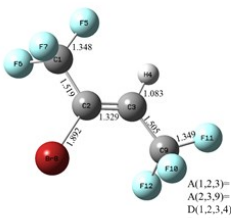

IMc6

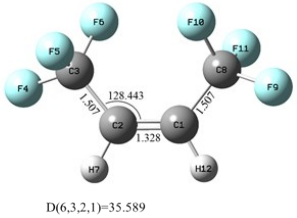

Pc3-2

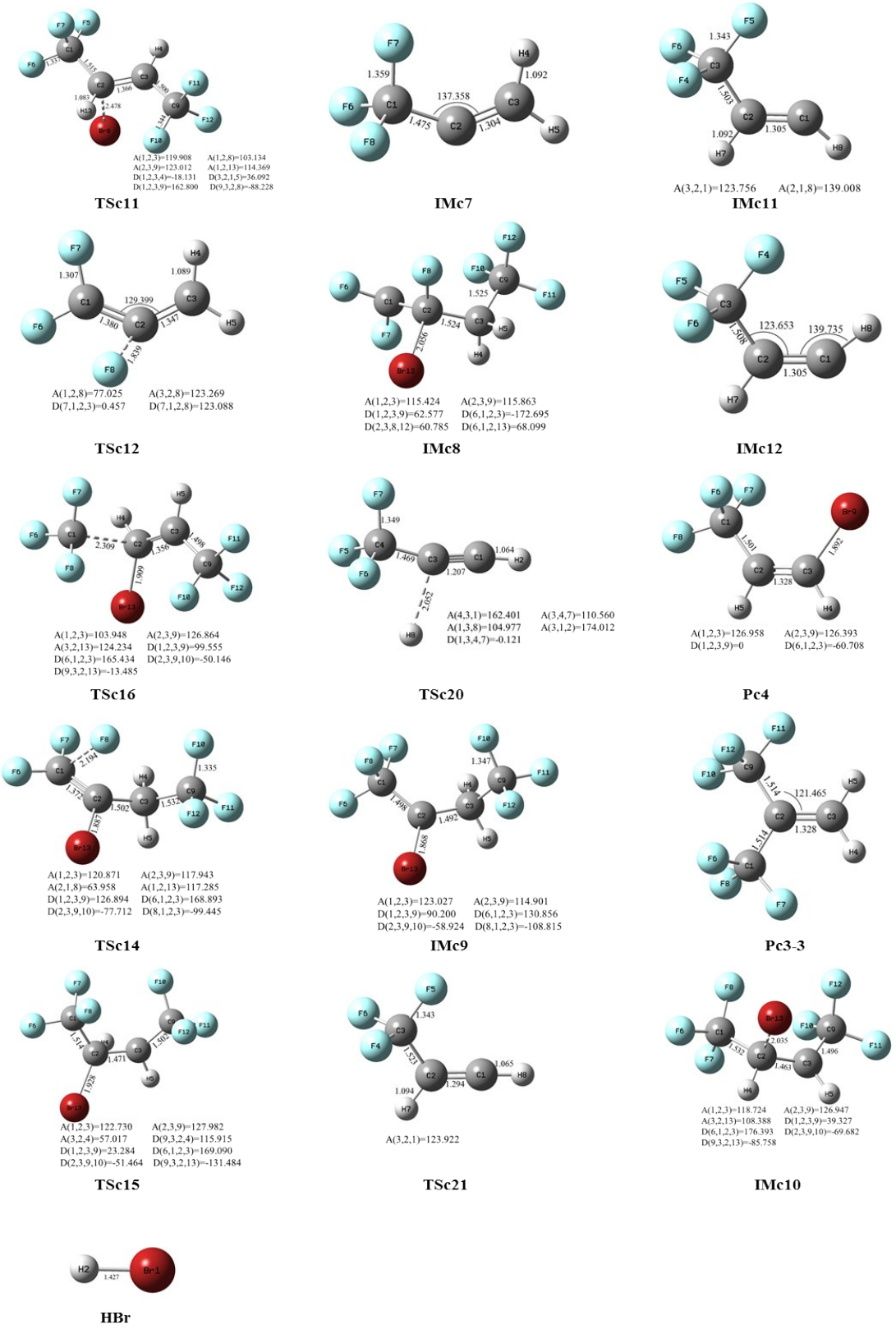

Figure S7. Geometric structures of main products, transition states and intermediate products in the optimal decomposition path of HCFO-1233xf and 2-BTP.

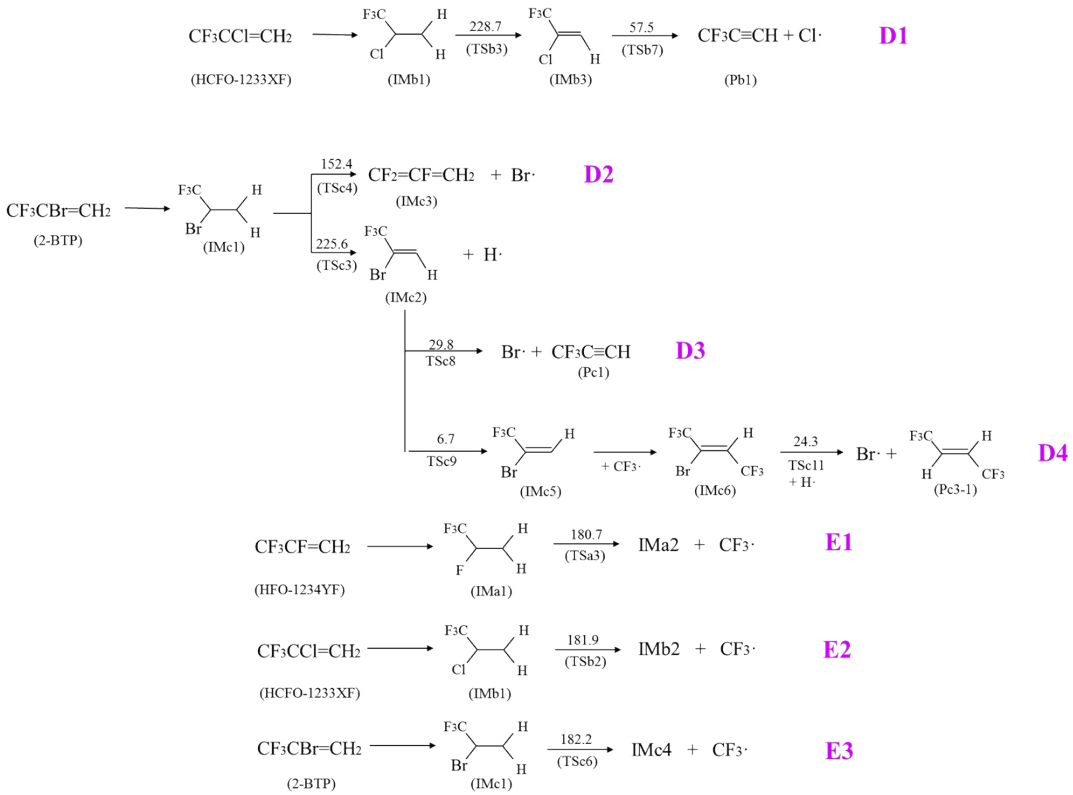

Figure S8. The schematic of generation of $Cl\cdot$, $Br\cdot$ and $CF_3\cdot$.

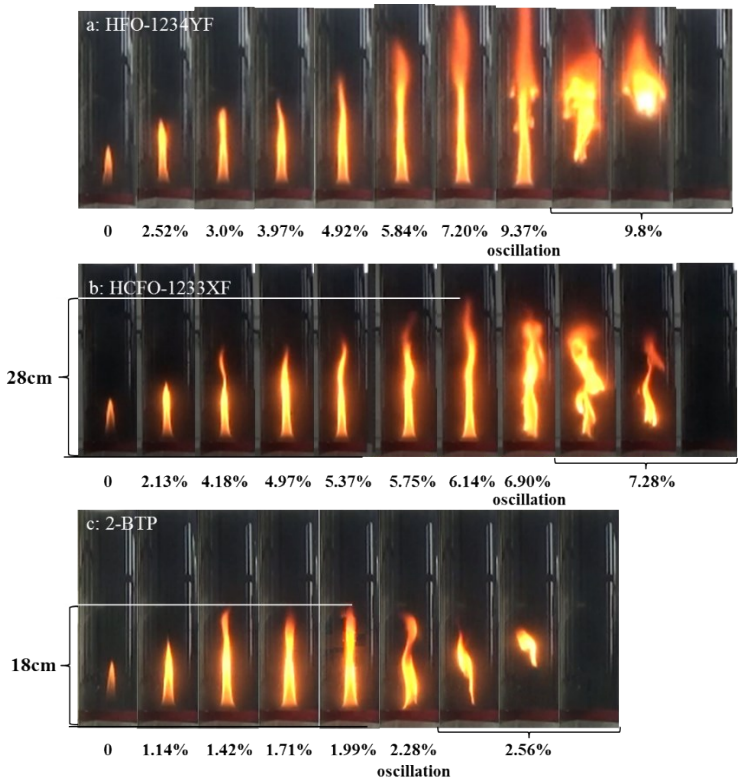

Figure S9. Methane-air flame appearance at different concentrations of (a) HFO-1234YF (b) HCFO-1233XF (c) 2-BTP.

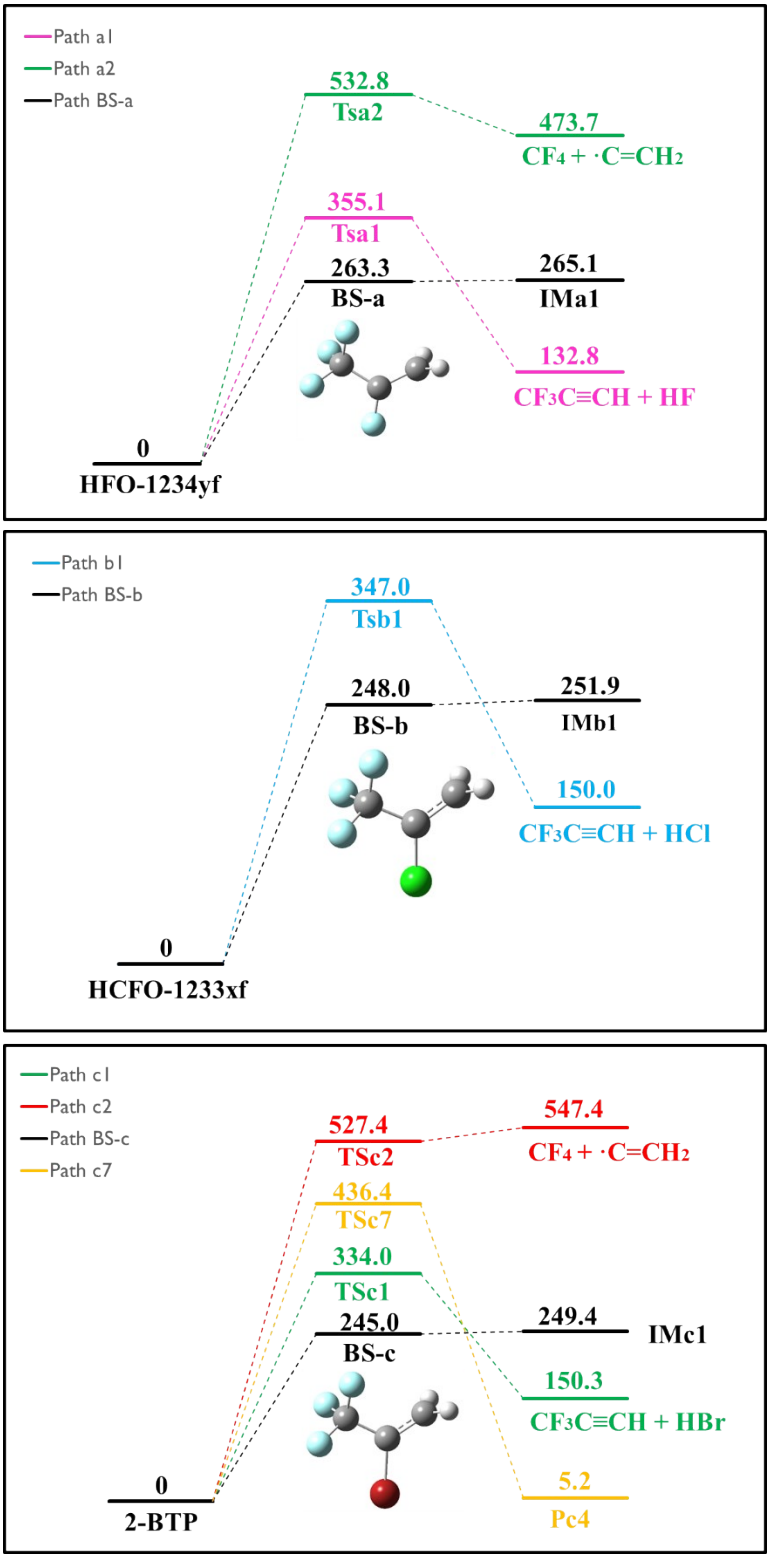

Figure S10. The potential energy diagram for the reaction pathways of first-step pyrolysis of HFO-1234yf, HCFO-1233xf and 2-BTP, calculated by using the M06-2X functional.

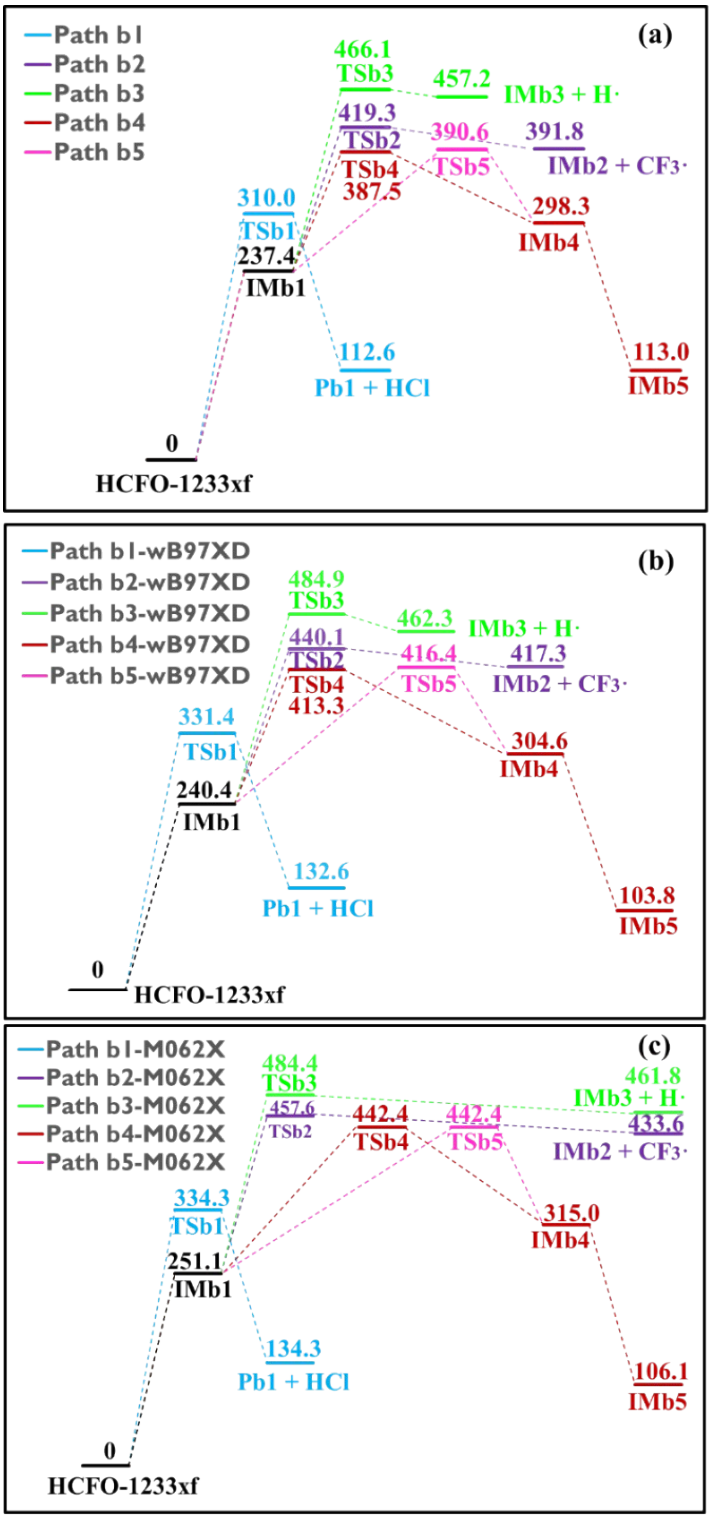

Figure S11. The potential energy diagram for the decomposition of HCFO-1233xf, calculated by using the (a) B3LYP, (b) wB97XD and (c) M06-2X functionals.

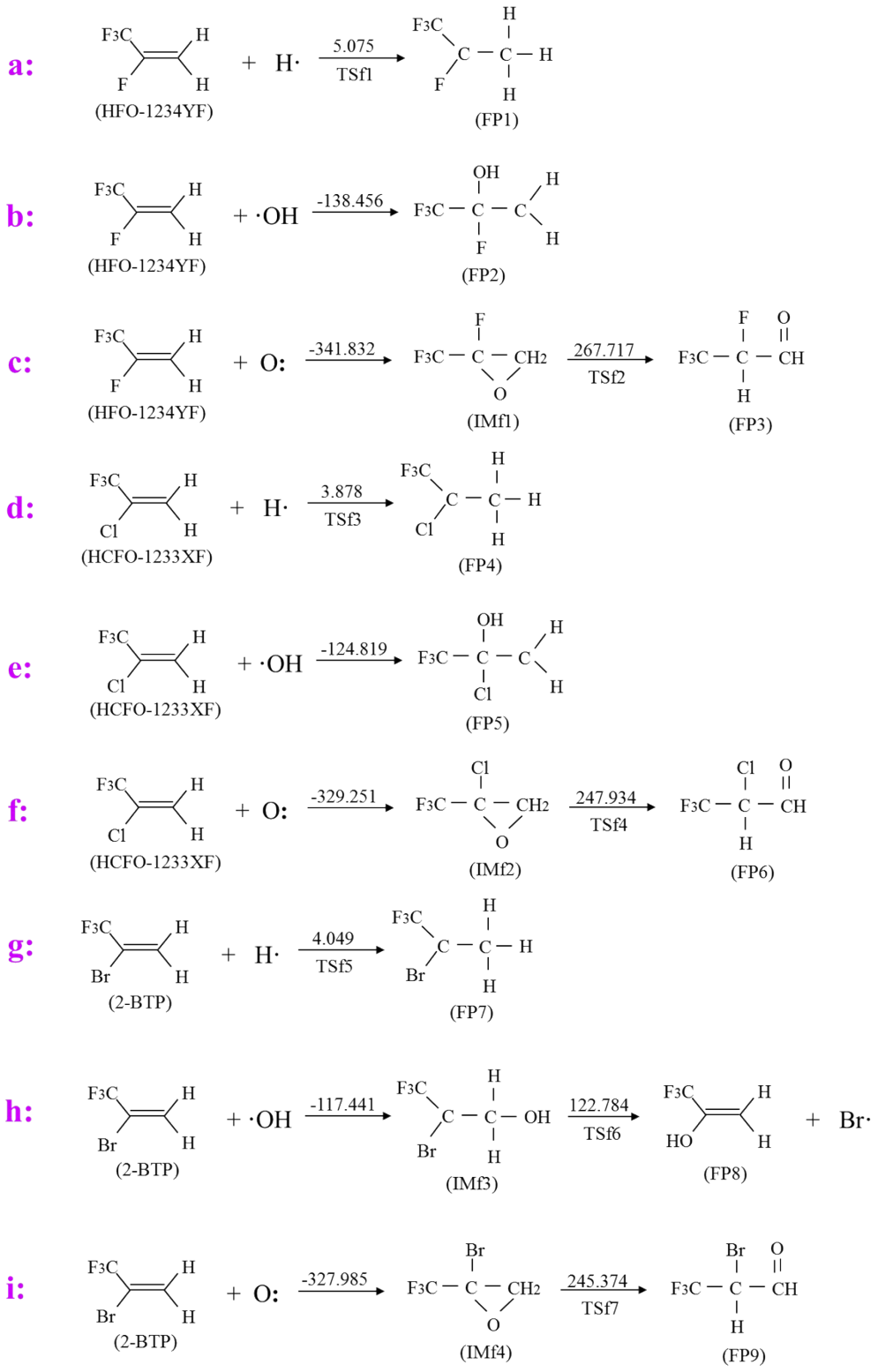

Figure S12. Pathways of reactions between the H•, OH• and O**:** free radicals and investigated HFO-1234YF, HCFO-1233XF and 2-BTP agents. The energy barrier is in the unit of kJ/mol.

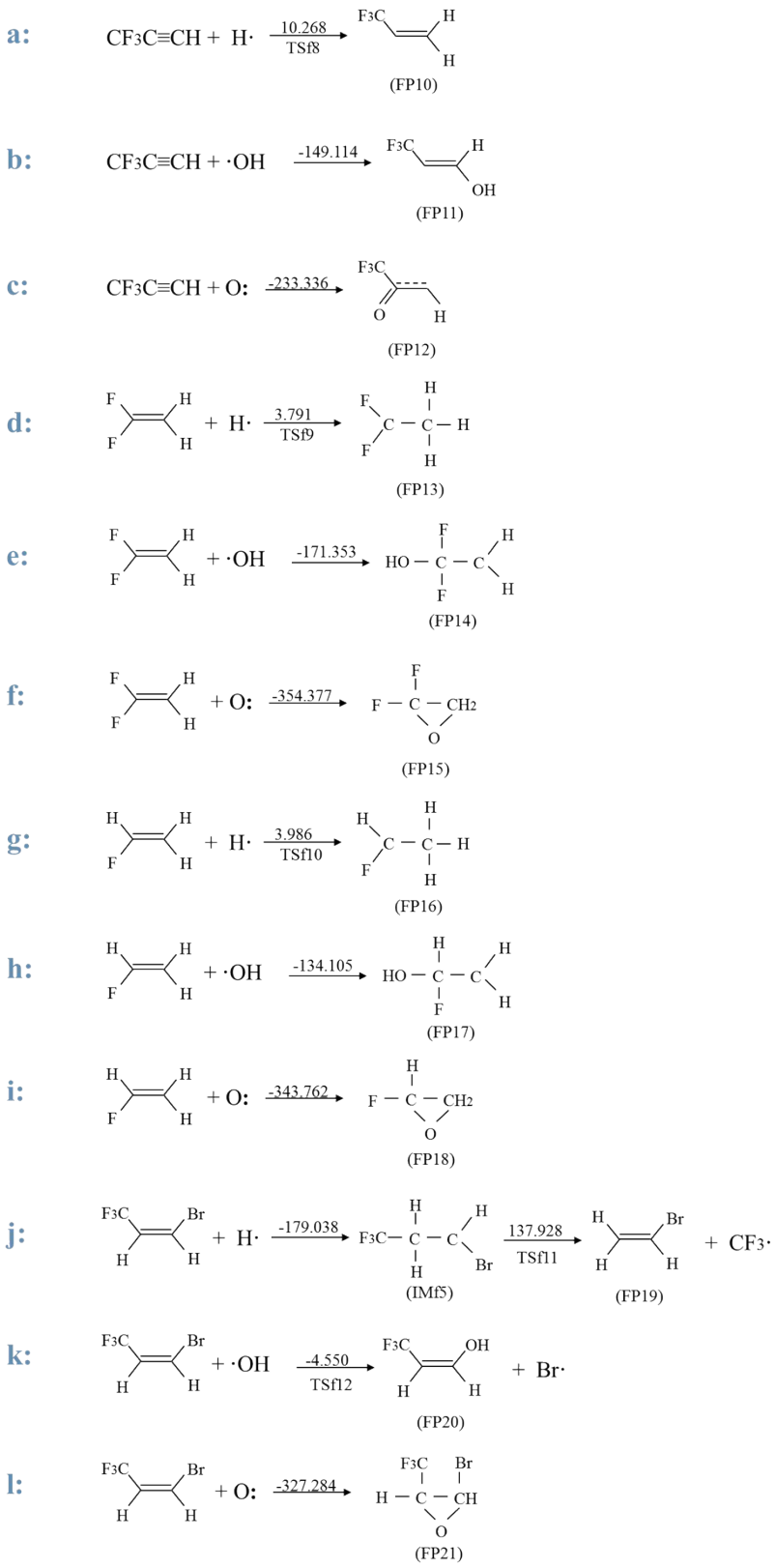

Figure S13. Reaction pathways of thermal decomposition products of HCFO-1233XF and HFO-1234YF in the flame with free radicals.

Table S1. Setting parameters for GC-MS

Parameters	GC-MS
Model number	Thermal Fisher Trace 1310
Chromatographic column	DBVRX, 30.0m, 0.25mm, 1.4μm
Flow rate of carrier gas	1.249 ml/min
Injection mode	15μL, gas, splitting mode
Split ratio	1:80
Injector temperature	280℃
Ion source temperature	240℃
Ionization methods	Electron bombardment
Ionizing energy	70eV
Scanned area	m/z 20-300

Table S2. BDEs of different bonds in HFO-1234yf molecule calculated at UB3LYP/6-311++G (d, p) level. The C-F bond at the middle carbon was highlighted by bold font. The S(S+1) value of •$CFCF_3$ and •CH_2 radicals equals to 2, and the S(S+1) value for other radicals is 0.75. The deviation between S(S+1) and $<S^2>$ locates at an acceptable range ($\Delta < 10\%$).

Bonds	Molecular Fragment	Ee + ZPE (Hartree)	$<S^2>$	BDEs[a] (kJ mol^{-1})	Bond distance (Å)
C-C	•CF_3	-337.658811	0.7517	408.722	1.509
	•$CF=CH_2$	-177.165581	0.7599		
C=C	•$CFCF_3$	-475.559668	2.0041	712.595	1.320
	•CH_2	-39.148985	2.0053		
C-F	•F	-99.76058	0.7513	443.142	1.349
	•$CF_2=CF=CH_2$	-415.050702	0.7759		
	•F	-99.76058	0.7513	443.142	1.347
	•$CF_2=CF=CH_2$	-415.050702	0.7759		
	•F	-99.76058	0.7513	443.137	1.345
	•$CF_2=CF=CH_2$	-415.050704	0.7759		
C-F	•F	-99.76058	0.7513	**483.000**	**1.346**
	•$CF_3C=CH_2$	-415.035521	0.7601		
C-H	•H	-0.502257	0.75	470.238	1.080
	•$CH=CFCF_3$	-514.298705	0.7597		
	•H	-0.502257	0.75	469.269	1.082
	•$CH=CFCF_3$	-514.299074	0.7601		
HFO-1234yf		-514.980066	---	---	---

Table S3. BDEs of different bonds in HCFO-1233xf molecule calculated at UB3LYP/6-311++G (d, p) level. The C-Cl bond at the middle carbon was highlighted by bold font. The S(S+1) value of •$CClCF_3$ and •CH_2 radicals equals to 2, and the S(S+1) value for other radicals is 0.75. The deviation between S(S+1) and $<S^2>$ locates at an acceptable range (Δ < 10%).

Bonds	Molecular Fragment	Ee + ZPE (Hartree)	$<S^2>$	BDEs[a] (kJ mol^{-1})	Bond distance (Å)
C-C	•CF_3	-337.658811	0.7517	391.769	1.512
	•$CCl=CH_2$	-537.528151	0.7599		
C=C	•$CClCF_3$	-835.928239	2.0063	679.886	1.325
	•CH_2	-39.148985	2.0053		
C-F	•F	-99.76058	0.7513	440.496	1.348
	•$CF_2=CCl=CH_2$	-775.407823	0.7774		
	•F	-99.76058	0.7513	440.496	1.348
	•$CF_2=CCl=CH_2$	-775.407823	0.7774		
	•F	-99.76058	0.7513	476.780	1.348
	•$CF_2=CCl=CH_2$	-775.394003	0.7527		
C-Cl	•Cl	-460.166882	0.7518	**351.229**	**1.745**
	•$CF_3C=CH_2$	-415.035521	0.7601		
C-H	•H	-0.502257	0.75	457.165	1.082
	•$CH=CClCF_3$	-874.659797	0.7611		
	•H	-0.502257	0.75	460.988	1.082
	•$CH=CClCF_3$	-874.658341	0.7611		
HCFO-1233xf		-875.336179	---	---	---

Table S4. BDEs of different bonds in 2-BTP molecule calculated at UB3LYP/6-311++G (d, p) level. The C-Br bond at the middle carbon was highlighted by bold font. The S(S+1) value of •$CBrCF_3$ and •CH_2 radicals equals to 2, and the S(S+1) value for other radicals is 0.75. The deviation between S(S+1) and $<S^2>$ locates at an acceptable range (Δ < 10%).

Bonds	Molecular Fragment	Ee + ZPE (Hartree)	$<S^2>$	BDEs[a] (kJ mol^{-1})	Bond distance (Å)
C-C	•CF_3	-337.658811	0.7517	387.309	1.511
	•$CBr=CH_2$	-2651.450612	0.76		
C=C	•$CBrCF_3$	-2949.851418	2.0074	673.535	1.325
	•CH_2	-39.148985	2.0053		
C-F	•F	-99.76058	0.7513	438.960	1.348
	•$CF_2=CBr=CH_2$	-2889.329168	0.7772		
	•F	-99.76058	0.7513	438.960	1.347
	•$CF_2=CBr=CH_2$	-2889.329168	0.7772		
	•F	-99.76058	0.7513	472.679	1.350
	•$CF_2=CBr=CH_2$	-2889.316325	-0.7532		
C-Br	•Br	-2574.105777	0.7515	**303.615**	**1.906**
	•$CF_3C=CH_2$	-415.035521	0.7601		
C-H	•H	-0.502257	0.75	455.514	1.081
	•$CH=CBrCF_3$	-2988.581186	0.7612		
	•H	-0.502257	0.75	449.207	1.083
	•$CH=CBrCF_3$	-2988.583588	0.7619		
	2-BTP	-2989.256939	---	---	---

Computational Details for the BDEs

The bond dissociation energies (BDEs) of molecules, which is energy consumed or released by breaking or forming a bond in a molecule, were calculated by using UB3LYP method. For instance, The BDE(C-C) is defined according the homolytic reaction ($CF_3CCl=CH_2 \rightarrow \bullet CF_3 + \bullet CCl=CH_2$) with the equation:

$$BDE(C\text{-}C) = [E_e(\bullet CF_3) + E_{ZPE}(\bullet CF_3)] + [E_e(\bullet CCl=CH_2) + E_{ZPE}(\bullet CCl=CH_2)] - [E_e(CF_3CCl=CH_2) + E_{ZPE}(CF_3CCl=CH_2)].$$

where E_e and E_{ZPE} denote the electronic energy and zero-point energy for these fragments/molecules of $\bullet CF_3$, $\bullet CCl=CH_2$ and $CF_3CCl=CH_2$. As recommended by the previous study, the UB3LYP method can give reliable results and the spin contamination $<S^2>$ locates at an acceptable range (< 10%), as listed in Table S2-S4.

Table S5. The Decomposition products and their preferable pathways of HFO-1234yf

Products	Preferable pathways
CF_3H	**A1'**: HFO-1234yf → IMa1 → TSa6 → IMa5 → IMa14 → TSa9 → IMa15 →Pa1
$CFH=CH_2$	**A2**: HFO-1234yf → IMa1 → TSa3 → IMa2 →Pa2
$CF_2=CH_2$	**A3'**: HFO-1234yf → IMa1 → TSa6 → IMa5 → TSa17 →IMa12 → TSa18 → IMa13 → Pa3
$CF_3CH=CHCF_3$(E)	**A4'**: HFO-1234yf → IMa1 → TSa6 → IMa5 → IMa14 → TSa19 → IMa15 → TSa20 → IMa16 → TSa21 → Pa4-1
$CF_3CH=CHCF_3$(Z)	**A4''**: HFO-1234yf → IMa1 → TSa4 → IMa3 → IMa6 → TSa11 → IMa7 → Pa4-2

Table S6. The decomposition products and their preferable pathways of HCFO-1233xf and 2-BTP

Substances	Products	Preferable pathways
HCFO-1233xf	$CF_3C{\equiv}CH$	**B1**: HCFO-1233xf → IMb1 → TSb3 → IMb3 → TSb7 → Pb1 + Cl•
2-BTP	$CF_3C{\equiv}CH$	**C1**: 2-BTP → IMc1 → TSc3 → IMc2 → TSc8 → Pc1 + Br•
	CF_3Br	CF_3•+ Br• → CF_3Br
	$CF_3CH{=}CHCF_3$(E)	**C3**: 2-BTP → IMc1 → TSc3 → IMc2 → TSc9 → IMc5 → IMc6 → TSc11 → Pc3-1 + Br• **C3'**: 2-BTP → IMc1 → TSc3 → IMc2 → TSc8 → Pc1 → TSc20 → IMc11 → TSc21 → IMc12 → Pc3-1
	$CF_3CH{=}CHCF_3$(Z)	**C3''**: 2-BTP → IMc1 → TSc3 → IMc2 → TSc8 → Pc1 → TSc20 → IMc11 → Pc3-2
	$(CF_3)_2C{=}CH_2$	**C3'''**: 2-BTP → IMc1 → TSc4 → IMc3 → TSc12 → IMc7 → Pc3-3
	$CF_3CH{=}CHBr$(Z)	**C4**: 2-BTP → IMc1 → TSc4 → IMc3 → IMc8 → TSc14 → IMc9 → TSc15 → IMc10 → TSc16 → Pc4 + CF_3•

Table S7. Energy barriers for the transition states of first-step pyrolysis reactions of $CF_3CX{=}CH_2$ (X = F, Cl, Br) substances. The TS states of BS-a, BS-b and BS-c represent the broken-symmetry states occurred in the generation of triplet states of IMa1, IMb1 and IMc1. All the energy barriers are in the unit of kJ/mol.

molecules	TS states	B3LYP	PBE0/cc-pVDZ	PBE0/6-311++G(d,p)	M06-2X/6-311G(d)
HFO-1234yf	**BS-a**	**364.7**	**242.1**	**239.1**	**263.3**
	TSa1	311.5	323.1	320.2	355.1
	TSa2	509.5	513.3	526.1	532.8
HCFO-1233xf	**BS-b**	**346.0**	**224.4**	**223.6**	**248.0**
	TSb1	310.0	320.3	324.0	347.0
2-BTP	**BS-c**	**336.7**	**220.5**	**219.5**	**245.0**
	TSc1	296.6	311.1	312.7	334.0
	TSc2	498.7	514.0	516.3	527.4
	TSc7	409.1	430.0	425.8	436.4